The effect of number of tube rows on optimal design of crimped spiral fin-and-tube heat exchangers

Parinya Kiatpachai[a], Anotai Suksangpanomrung[a], Phubate Thiangtham[b], Chanyoot Keepaiboon[b], Weerapun Duangthongsuk[c], Somchai Wongwises[d*]

[a]Department of Mechanical Engineering, Academic Division, Chulachomklao Royal Military Academy, Nakhon Nayok 26001, Thailand

[b]Thai-Ingenieur Co., Ltd, Bangkok, 10510, Thailand

[c]Department of Mechanical Engineering, Southeast Asia University, Bangkok, Thailand

[d]Fluid Mechanics, Thermal Engineering and Multiphase Flow Research Lab. (FUTURE), Department of Mechanical Engineering, Faculty of Engineering, King Mongkut's University of Technology Thonburi, Bangmod, Bangkok 10140, Thailand

*Corresponding author: somchai.won@kmutt.ac.th

Abstract The aim of this study is to optimize the number of tube rows (N_{row}) of crimped spiral fin–and-tube heat exchangers. Multipass parallel-and-counter cross-flow heat exchangers are used to study this topic. As the working fluids, ambient air was used at the air side, whereas hot water was used at the tube side. We demonstrated that the Nrow has no significant effect on the j and f factors, especially the optimal number of tube rows (N_{row}) for crimped spiral fins with 3 and 4 rows, based on the $\zeta 1$, $\zeta 2$, and $\zeta 3$ evaluation criteria. The major findings related to those effects are also described in this study. The results showed certain aspects of other effects for enhancing our understanding on effective heat-exchanger design.

Keywords**:** tube, fin, heat transfer, heat exchanger, number of tube row

1. Introduction

Air-side heat-transfer performance is very important to heat exchanger (HX) design at a compact size, which is generally limited by the air-side resistance. Therefore, fin geometry and tube arrangements have been improved to enhance the heat transfer in heat exchangers.

A literature survey reveals that many researchers have studied extensively about how fin geometries and tube arrangements affect the air-side heat-transfer performance and flow characteristics of plate-and-circular-finned-tube HXs, as reviewed by Pongsoi et al. [1]. Moreover, there has a limited number of studies on the air-side performance of HX designs with conventional spiral fins [2-10], crimped spiral fins [11-13], L-footed spiral fins [14-16], and serrated welded spiral fins [17]. They showed that the conventional spiral fin is the foundation of other spiral fins, as seen in Fig. 1. Several of the spiral fin types differ from the conventional spiral fin mainly in terms of the fin base. In particular, crimped spiral fins have a sine shape, which increases the contact area between the fin base and tube surface as well as the turbulent flow. An L - footed spiral fin can protect against corrosion through the base of its (L-shaped) fin, whereas a welded spiral fin has lower thermal resistance than other fin types do but also high heat-transfer performance and pressure drop. In addition, according to the literature, the resulting air-side performance has significant effects on HX design, leading to improved fin geometry and tube arrangements. Designers must use the majority of these method-development experiments to enhance the understanding of effective HX design. In order to match the real applications, as a result, this study will focus on the optimal design of tube banks by using Wongwises's research group and considering performance indexes, as reported in Pongsoi et al. [11-16] and Kiatpachai et al. [17]. Additionally, crimped spiral fin-and-tube HXs with 2-5 rows are studied using performance indexes for the optimal design of tube banks. This work also has guided Nrow for designing crimped, spiral-finned-tube HXs in industrial applications, which can be applied to future technology.

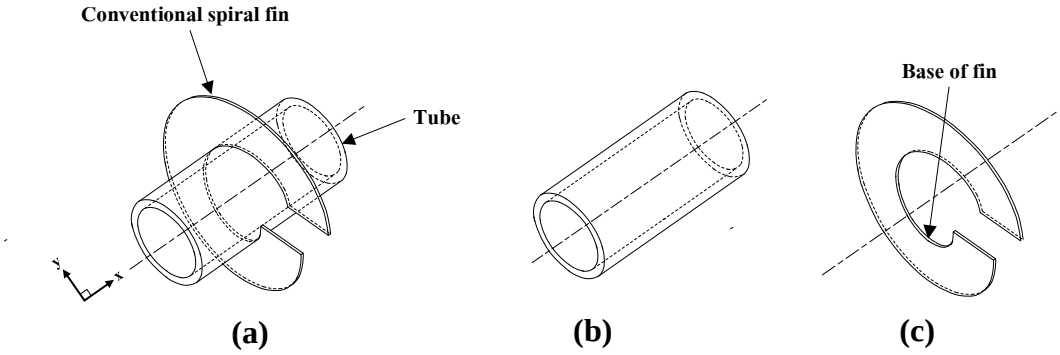

Fig.1 Schematic diagrams for (a) conventional spiral-finned tubes, (b) tubes, and (c) conventional spiral fins [From Pongsoi et al. [1], with permission from Elsevier]

2. Data Reduction

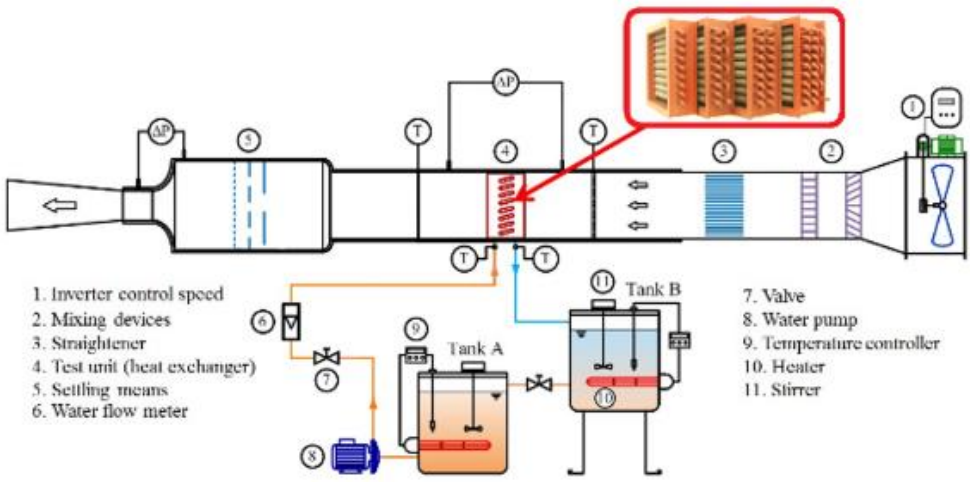

Fig.2 Schematic diagrams of the experimental apparatus [From Pongsoi et al. [13], with permission from Elsevier]

An experiment was operated in a wind tunnel, as seen in Fig.2 The main components of the experimental apparatus are the spiral fin–and-tube HX (test section), data-acquisition system, instrument system, water flow loop, and air supply. The working fluids used for the experiment were air and hot water.

Fig. 3 shows the crimped finned tube used for the experiment. The schematic diagrams of all parameters of the tested HXs are shown in Fig. 4 Moreover, Table 1 provides details of the test samples. The relevant components and more detailed descriptions can be seen in a previous study [18]. For out experiment, the air and water flow rates and water temperatures were varied for testing at the steady state, as seen in Table 2. The NTU method and total thermal resistance are used for data reduction for UA product under steady-state conditions, which can be represented as follows:

$$\frac{1}{UA} = \frac{1}{h_i A_i} + \frac{\ln(d_o/d_i)}{2\pi k_t L} + \frac{1}{\eta_o h_o A_o} \quad (1)$$

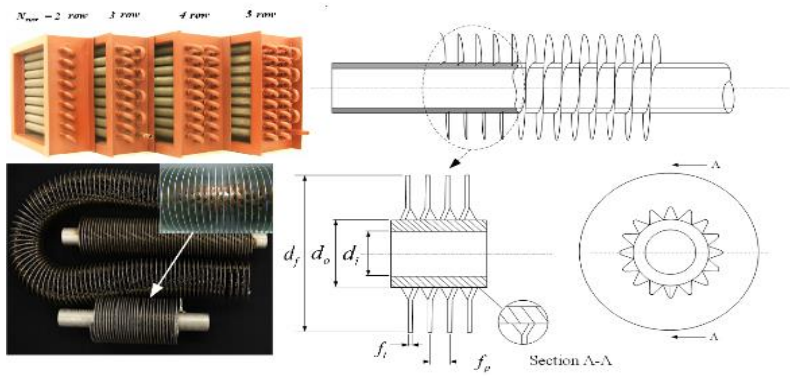

Fig.3 Photos and schematic diagrams of the crimped spiral-finned tube[From Pongsoi et al. [11], with permission from Elsevier]

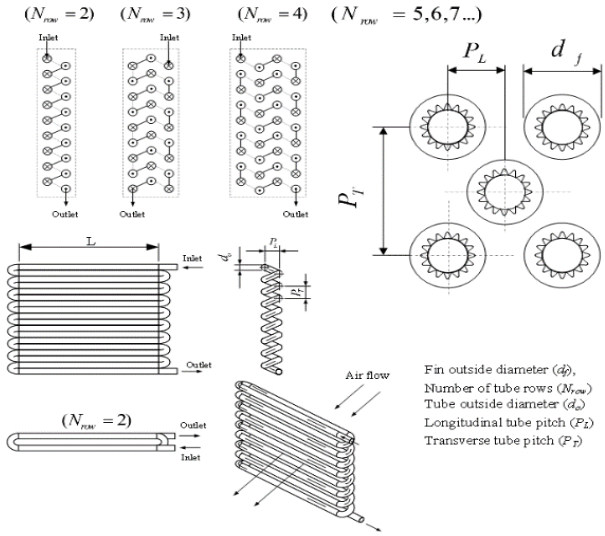

Fig.4 Crimped spiral-fin-and-tube HXs [From Pongsoi et al. [12], with permission from Elsevier]

Table.1 Detailed geometric parameters of the test samples

No.	d_i	d_o	d_f	P_L	P_T	f_t	n_t	f_p	Fin material	N_{row}
1,2,3,4	13.5	16.35	35	35	40	0.5	9	6.3	*Al*	2,3,4,5

Unit: mm

Table.2 Experimental conditions

Inlet-air dry-bulb temperature, ^{O}C	31.5±0.5
Inlet-air frontal velocity, *m/s*	2-7
Intel-water temperature, ^{O}C	55-70
Water flow rate, *LPM*	12-14

Table.3 Accuracy of the measurements

Parameters	Accuracy
Inlet-air dry-bulb temperature, ^{O}C	±0.1
Pressure drop, *Pa*	±0.5
Intel-water temperature, ^{O}C	±0.1
Water flow rate, *kg/s*	±0.4

Table.4 Uncertainties of the derived experimental values

Parameters	Maximum uncertainties (%)
Air-side heat transfer rate, Q_o	±5.0
Water-side heat transfer rate, Q_w	±3.4
Pressure drop, ΔP	±2.5
Frontal velocity, V_{fr}	±3.3
Colburn factor, j	±11.5
Friction factor, f	±13.0

Equations (2)-(9), for one mixed fluid and one unmixed fluid, were used to determine ho, as follows:

For a multipass parallel cross-flow with N_{row}= 2, 3, 4, and 5 or higher:

(N_{row} = 2),

$$\varepsilon_P = \left(1-\frac{K}{2}\right)\left(1-e^{-2K/C_A^*}\right), K = 1-e^{-NTU_A(C_A^*/2)} \tag{2}$$

(N_{row} = 3)

$$\varepsilon_P = 1-\left(1-\frac{K}{2}\right)^2 e^{-3K/C_A^*} - K\left[1-\frac{K}{4}+\frac{K}{C_A^*}\left(1-\frac{K}{2}\right)\right]e^{-K/C_A^*}, K = 1-e^{-NTU_A(C_A^*/3)} \tag{3}$$

(N_{row} = 4),

$$\varepsilon_P = 1-\frac{K}{2}\left(1-\frac{K}{2}+\frac{K^2}{4}\right)-K\left(1-\frac{K}{2}\right)\left(1+2\frac{K}{C_A^*}\left[1-\frac{K}{2}\right]\right)e^{-2K/C_A^*}-\left(1-\frac{K}{2}\right)^3 e^{-4K/C_A^*}, K = 1-e^{-NTU_A(C_A^*/4)} \tag{4}$$

(N_{row} = 5 or ∞),

$$\varepsilon_P = \frac{1-e^{-NTU_A(1+C_A^*)}}{1+C_A^*} \tag{5}$$

For multipass counter cross-flow with N_{row}= 2, 3, 4 and 5 or more:

(N_{row} = 2),

$$\varepsilon_c = 1-\left[\frac{K}{2}+\left(1-\frac{K}{2}\right)e^{2K/C_A^*}\right]^{-1}, K = 1-e^{-NTU_A(C_A^*/2)} \tag{6}$$

(N_{row} = 3),

$$\varepsilon_c = 1-\left\{\left(1-\frac{K}{2}\right)^2 e^{3K/C_A^*}+\left[K\left(1-\frac{K}{4}\right)-\left(1-\frac{K}{2}\right)\frac{K^2}{C_A^*}\right]e^{K/C_A^*}\right\}^{-1}, K = 1-e^{-NTU_A(C_A^*/3)} \tag{7}$$

(N_{row} = 4),

$$\varepsilon_c = 1-\left[\frac{K}{2}\left(1-\frac{K}{2}+\frac{K^2}{4}\right)+K\left(1-\frac{K}{2}\right)\left[1-2\frac{K}{C_A^*}\left(1-\frac{K}{2}\right)\right]e^{2K/C_A^*}+\left(1-\frac{K}{2}\right)^3 e^{4K/C_A^*}\right]^{-1}, K = 1-e^{-NTU_A(C_A^*/4)} \tag{8}$$

(N_{row} = 5 or ∞),

$$\varepsilon_c = \frac{1-e^{-NTU_A(1-C_A^*)}}{1-C_A^* e^{-NTU_A(1-C_A^*)}} \tag{9}$$

The heat capacity-rate ratio ($C^* = C_{min}/C_{max}$) represents C_c/C_h or C_h/C_c:

$$\varepsilon_{pc} = \frac{\varepsilon_P + \varepsilon_C}{2} \quad \text{for } N_{row} = 2, 3, 4 \text{ and } 5 \tag{10}$$

The radial fin efficiency is proposed by Gardner [19]:

$$\eta_f = \frac{2\psi}{\phi(1+\psi)}\frac{I_1(\phi R_o)K_1(\phi R_i) - I_1(\phi R_i)K_1(\phi R_o)}{I_0(\phi R_i)K_1(\phi R_o) + I_1(\phi R_o)K_0(\phi R_i)} \tag{11}$$

Where

$$\phi = (r_o - r_i)^{3/2}\left(\frac{2h_o}{k_f A_p}\right)^{1/2} \tag{12}$$

The Colburn j factor presents the heat-transfer performance of forced convection:

$$j = \frac{Nu}{\mathrm{Re}_{do}\,\mathrm{Pr}^{1/3}} = \frac{h_o}{\rho_a V_{\max} c_P}(\mathrm{Pr})^{2/3} \tag{13}$$

The 3 performance indexes are presented to determine the optimal number of tube rows, as reported in [13]. The values of ζ1, ζ2, and ζ3 are determined as follows in (14)-(16):

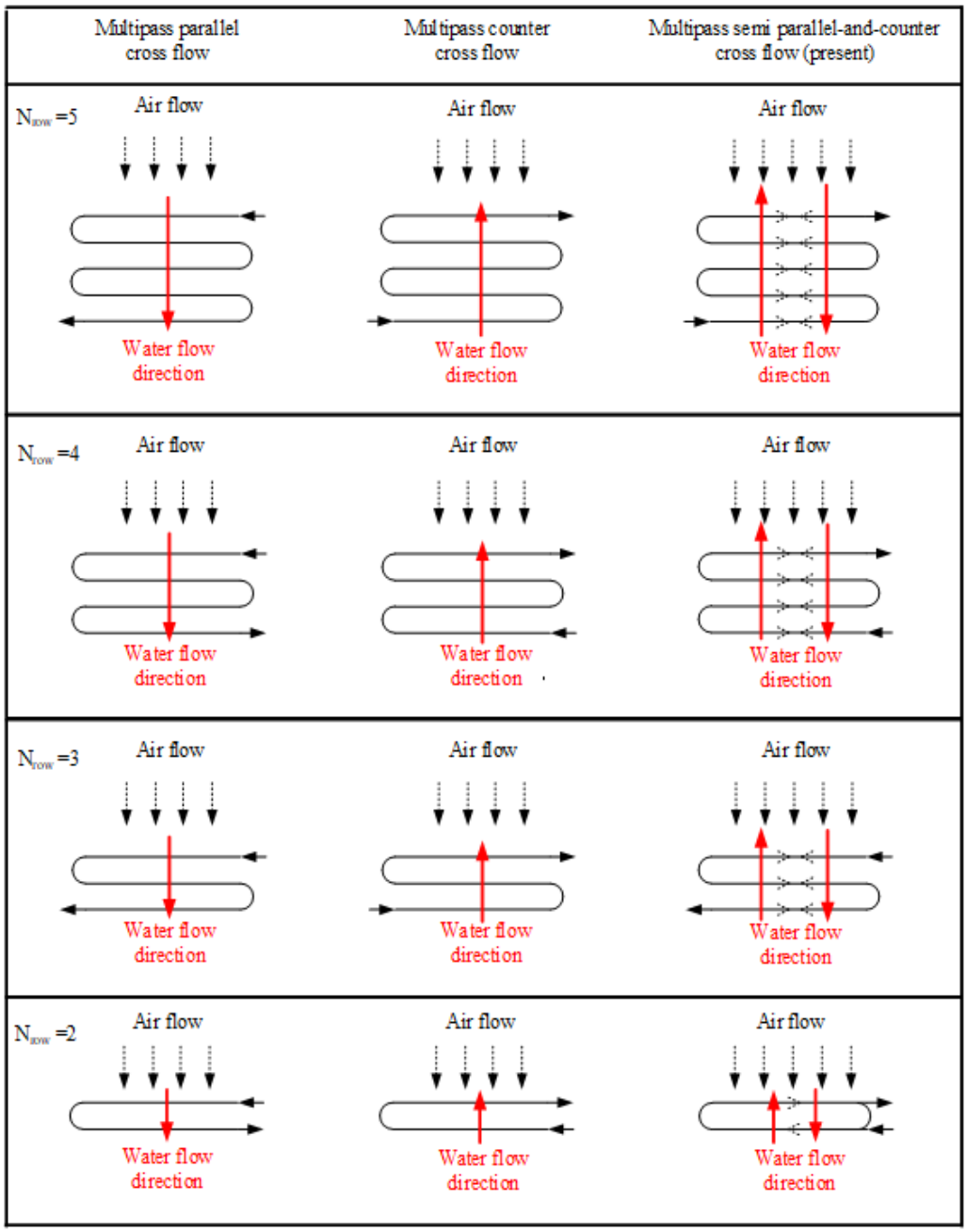

Fig.5 Schematic diagram of the heat-exchanger algorithm for multipass parallel cross-flow, multipass counter cross-flow, and multipass parallel and counter cross-flow (N_{row} = 2, 3, 4, and 5)

The HX performance index is calculated as follows:

$$\zeta 1 = (Q_{ave}/\Delta P)_{HX} \quad (14)$$

The system-performance index is calculated as follows:

$$\zeta 2 = (Q_{ave}/\Delta P)_{Sys} \quad (15)$$

The dimensionless system-performance index is calculated as follows:

$$\zeta 3 = (Q_{ave}/W_p)_{Sys}, \quad (16)$$

in which W_p is the fan power.

The pumping power of fan was determined Kays and London [20], as described in more detail in [13], as follows:

$$W_p = \frac{G_c A_{min} \Delta P}{\rho_m} \quad (17)$$

3. Results and Discussion

The ANSI/ASHRAE 33 Standards [21] were used to identify the energy balance, which was $|Q_a-Q_w| / Q_{ave}$. < 0.05 Moreover, the accuracy and uncertainties of the derived experimental values are provided in Tables 3 and 4, respectively.

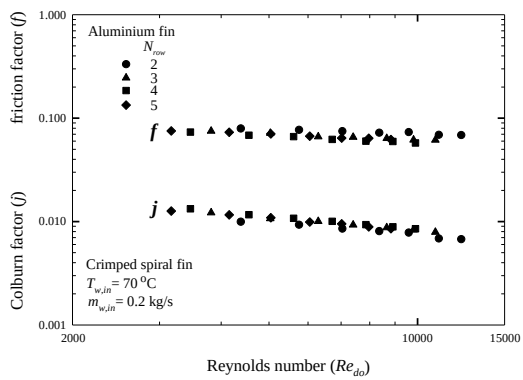

Fig.6 Effect of number of tube rows on the j and f factors of crimped spiral fin and tube heat-exchangers at $T_{w,in}$= 70 °C and $m_{w,in}$= 0.2 kg/s.

Fig.6 shows the effects of N_{row} on heat-transfer performance and flow characteristics in term of the j and f factors. The j and f factors decrease as Redo increases (3,000-15,000).

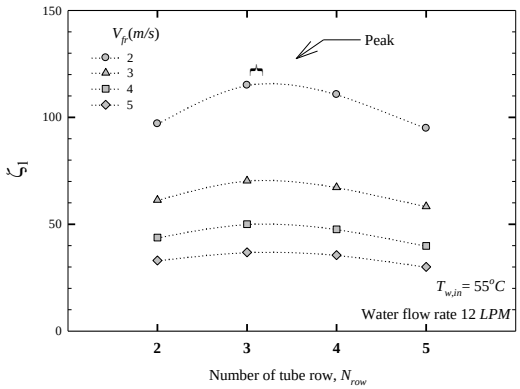

(a)

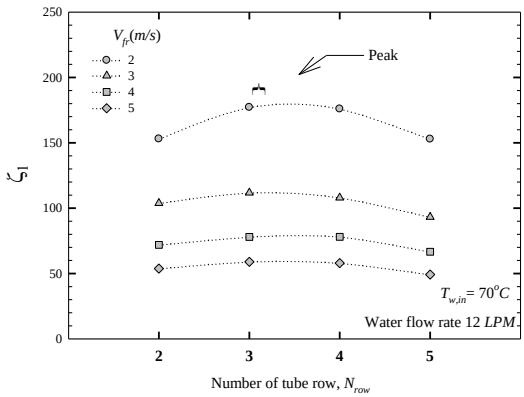

(b)

Fig.7 Effect of number of tube rows on the heat-exchanger performance index ζ_1 at different inlet-water temperatures: (a) 55 °C/12 LPM and (b) 70 °C/12 LPM

This might be because the downstream turbulence is shed, passing the finned-tube HX and leading to good mixing at the air side. In contrast, N_{row} has a significant

effect on flow characteristics, as seen in terms of f. The effect of blocking the flow area increases with the number of tube rows.

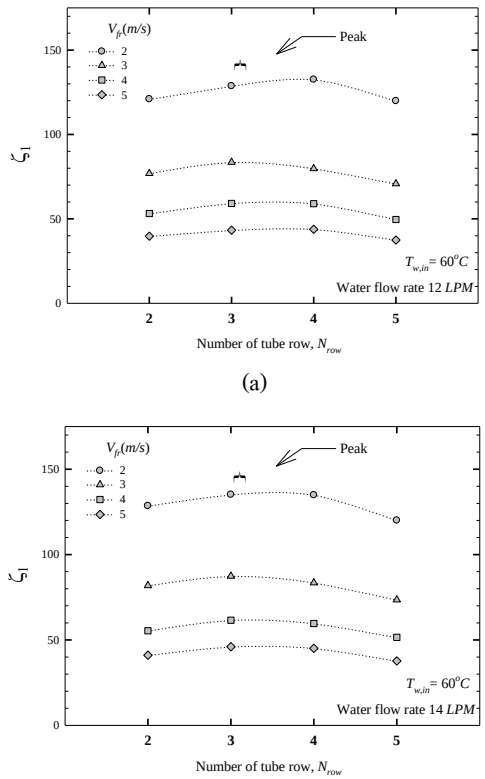

Fig.8 Effect of number of tube rows on the heat-exchanger performance index ζ_1 at different water flow rates: (a) 60 °C/12 LPM and (b) 60 °C/14 LPM

The analysis of N_{row} for HX design is presented using 3 performance indexes [13]: ζ_1, ζ_2, and ζ_3, as expressed in Eqs. (14), (15), and (16), respectively. Figs. 7 and 8 illustrate the HX performance index (ζ_1) with 2-5 tube rows at various temperatures and a flow rate of water and air frontal velocity of 2-5 m/s. The results demonstrate that ζ_1 when N_{row} is 3 or 4 rows (the peak values) is higher than that when N_{row} is 2 or 5 rows.

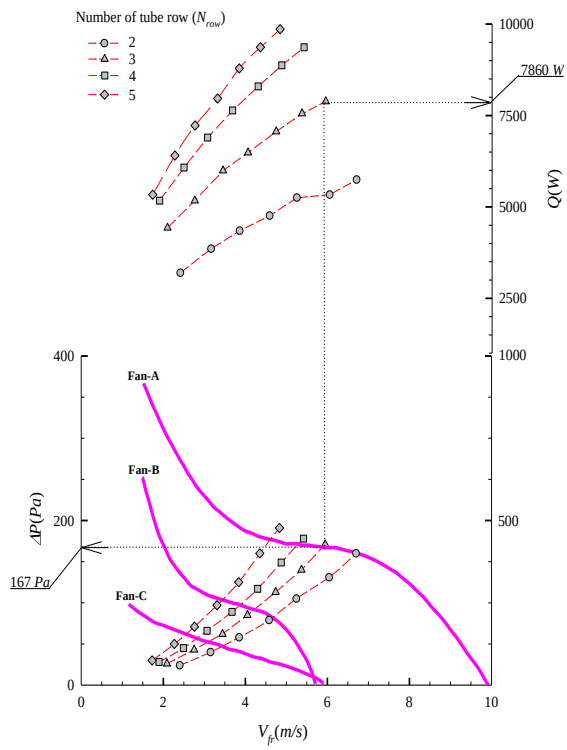

Fig.9 Axial fan-performance curve (P-Q fan curve) with system lines of L-footed spiral fin-and-tube heat exchangers with various numbers of tube rows at $T_{w,in}$ = 70 °C and water flow rate of 12 LPM

Thus, N_{row} of 3 and 4 rows was used for optimum design based on the HX performance index (ζ_1).

Fig. 9 illustrates the P-Q curve of axials fan with the system lines of HXs having 2-5 tube rows. The P-Q curve A to C of a commercial fan is plotted to determine the cutting line between the fan curve and the HX's system line, i.e., the operating point. The interception of the 2 operating points shows the average heat transfer rate and pressure drop when Nrow is 3 and with fan A. The value ζ_2 is the ratio of Q_{ave} with the ΔP at the operating point, as shown in Fig. 9.

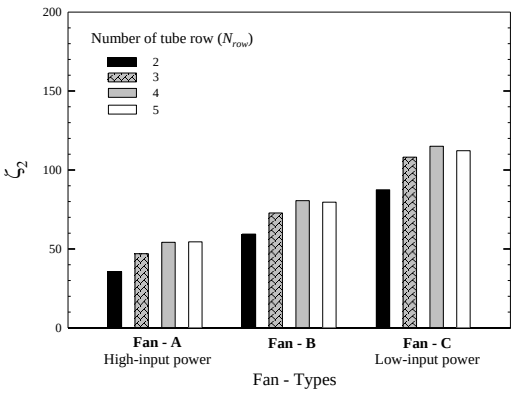

Fig.10 Effect of the number of tube rows subjected to the fan curve on the performance index ζ_2 at the optimum fan-operating point ($T_{w,in}$ = 70 °C and water flow rate of 12 LPM)

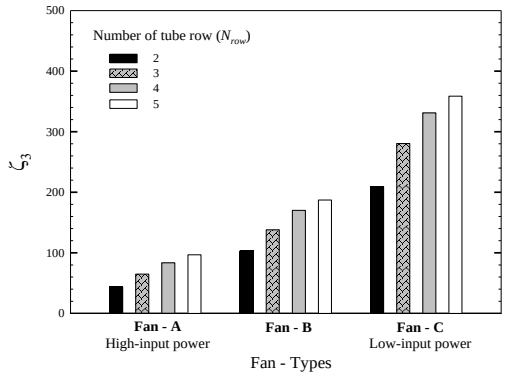

Fig.11 Effect of number of tube rows subjected to pumping (fan) power on the performance index ζ_3 at the optimum fan-operating point ($T_{w,in}$ = 70 °C and water flow rate of 12 LPM)

The influence of number of tube rows for crimped spiral fins in relation to the fan curve on ζ_2 at the optimum fan-operating point is illustrated in Fig. 10. The system-performance index (ζ_2) increases when N_{row} increases to 2 to 4 rows, but N_{row} = 5 has a decreased ζ_2 , as seen in Fig. 10. The plots of the dimensionless system-performance index (ζ_3) shown in Fig. 11 show the same trend as that of ζ_2. These performance indexes are compared for N_{row} of 2, 3, 4, and 5 rows, as seen in Table .5

Table.5 Characteristics of N_{row} on the performance indexes

N_{row}	ζ_1	ζ_2	ζ_3
2	Low	Low	Low
3*	High*	Intermediate*	Intermediate*
4*	High*	High*	Intermediate*
5	Low	Intermediate	High

Note: *Optimum condition

We confirmed that N_{row} of 3 and 4 rows was significantly better than other numbers of tube rows were, which we investigated by the intersection method, as shown in Fig. 12. A previous study, Pongsoi et al. [13], noted that the optimum fin pitch was 4.2 mm (crimped spiral fin), making it suitable for effective HX design.

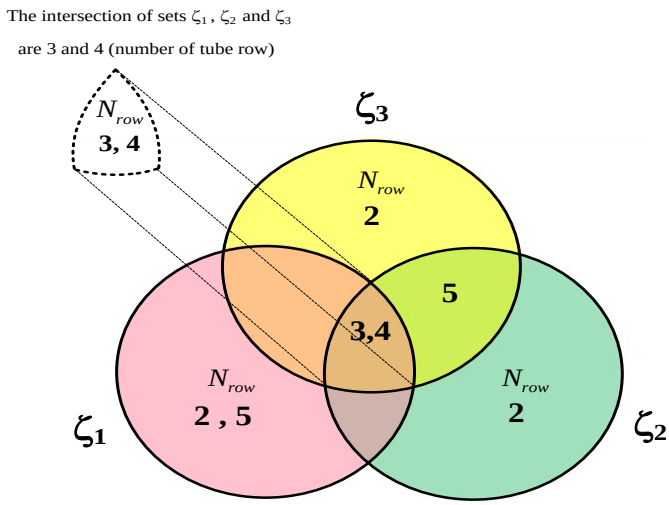

Fig.12 The levels of 3 performance index sets (ζ_1, ζ_2, and ζ_3) as the grouping of the number of tube rows

4. Conclusion

To summarize, the optimal design for a crimped spiral fin–and–tube HX involves the effect of N_{row} (2-5 rows), which was considered by using 3 performance indexes (ζ_1, ζ_2, and ζ_3). The findings were as follows:

1. N_{row} affects the heat-transfer performance and flow characteristics of an optimal HX design.
2. The value of N_{row} for crimped spiral fin–and-tube HXs is summarized for industrial application design, i.e., N_{row} of 3 or 4 rows at a high Reynolds number.
3. The most effective design of a spiral fin–and-tube HX is challenging to discover, create, design, investigate, and apply to innovation technology, to lead to new types of HXs.

Acknowledgments

The authors would like to thank Department of Mechanical Engineering, Academic Division, Chulachomklao Royal Military Academy (CRMA), Chulachomklao Royal Military Academy Development Fund and the Department of Mechanical Engineering, Faculty of Engineering, King Mongkut's University of Technology Thonburi (KMUTT) for supporting this study.

Nomenclatures

A	area, m^2
A_{min}	minimum free flow area, m^2
A_o	total surface area, m^2
A_P	cross-sectional or profile area of fin, m^2
Al	aluminium
c_P	specific heat at constant pressure, J/(kg.K)
C	heat capacity rate, *W/K*
C^*	capacity rate ratio, dimensionless

C_c	cold-fuid capacity rate, W/K
C_h	hot-fluid capacity rate, W/K
Cu	copper material
d_f	outside diameter of finned tube, m
d_i	tube inside diameter, m
d_o	tube outside diameter, m
f	Fanning friction factor
f_p	fin pitch, m
f_t	fin thickness, m
G_c	mass flux of the air based on minimum free flow area, kg/m^2.s
H	height, m
HX	heat exchanger
h	heat transfer coefficient, W/(m^2.K)
I_0	modified Bessel function solution of the first kind, order 0
I_1	modified Bessel function solution of the first kind, order 1
j	Colburn factor
k	thermal conductivity, W/(m.K)
K_0	modified Bessel function solution of the second kind, order 0
K_1	modified Bessel function solution of the second kind, order 1
L	length, m
LPM	litre per minute
m	mass flow rate, kg/s; fin performance parameter, m^{-1}
N_{row}	number of tube rows
NTU	number of transfer units, dimensionless
P_L	longitudinal tube pitch, m
Pr	Prandtl number
P_T	transverse tube pitch, m
Q	heat transfer rate, W
r_o	radius of tip fin, m
r_i	radius of base fin, m
R	radius function in terms of the radius ratio, dimensionless
Re_{di}	Reynolds number based on tube inside diameter
Re_{do}	Reynolds number based on tube outside diameter
T	temperature, ^{o}C
T_a	air temperature, ^{o}C
T_w	water temperature, ^{o}C
U	overall heat transfer coefficient, W/(m^2.K)
V_{fr}	frontal velocity, m/s
V_{max}	maximum velocity across heat exchanger, m/s

Greek symbols

ε	heat exchanger effectiveness
η	fin efficiency
η_o	overall surface effectiveness
ρ	density, kg/m^3
σ	contraction ratio of cross-sectional area
μ	dynamic viscosity of air, Pa.s
ϕ	combination of terms, dimensionless;
ψ	radius ratio
ΔP	pressure drop, *Pa*
ζ_1	heat exchanger performance index, *W/Pa*
ζ_2	system performance index, *W/Pa*
ζ_3	dimensionless system performance index, dimensionless

Subscripts

1	air-side inlet
2	air-side outlet
a	air
ave	average
b	base
c	multipass counter cross flow or cold fluid
f	fin
fr	frontal (LxH)
h	hot fluid
i	tube-side
in	inlet
m	mean value
max	maximum
o	air-side
p	multipass parallel cross flow
pc	multipass parallel-and-counter cross flow
out	outlet
t	tube
w	water

References

[1] P. Pongsoi, S. Pikulkajorn, S. Wongwises, "Heat transfer and flow characteristics of spiral fin-and-tube heat exchangers: A review," *International Journal of Heat and Mass Transfer,* Vol.79, pp.417-431, 2014.

[2] H. Hamakawa, K. Nakashima, T. Kudo, E. Nishida, T. Fukano, "Vortex Shedding from a Circular Cylinder with Spiral Fin," *J. of Fluid Science and Technology,* Vol.3, pp.787-795, 2008.

[3] M. Lee, T. Kang, Y. Kim, "Air-side heat transfer characteristics of spiral-type circular fin-tube heat exchangers," *Int. Journal of Refrigeration,* Vol.33, pp.313-320, 2010.

[4] M. Lee, T. Kang, Y. Joo, Y. Kim, "Heat transfer characteristics of spirally-coiled circular fin-tube heat exchangers operating under frosting conditions," *Int. Journal of Refrigeration*, Vol.34, pp.328-336, 2011.

[5] H. FaJiang, C. WeiWu, Y. Ping, "Experimental Investigation of Heat Transfer and Flowing Resistance for Air Flow Cross over Spiral Finned Tube Heat Exchanger," *Energy Procedia*, Vol.17, pp.741-749, 2012.

[6] S.B. Genic, B.M. Jacimovic, B.R. Latinovic, "Research on air pressure drop in helically-finned tube heat exchangers," *Applied Thermal Engineering,* Vol.26, pp.478-485, 2006.

[7] M. Lee, T. Kang, Y. Kim, "Air-side heat transfer characteristics of spiral-type circular fin-tube heat exchangers," *Int. Journal of Refrigeration,* Vol.33, pp.313-320, 2010.

[8] M. Lee, T. Kang, Y. Joo, Y. Kim, "Heat transfer characteristics of spirally-coiled circular fin-tube heat exchangers operating under frosting conditions," *Int. Journal of Refrigeration,* Vol.34, pp.328-336, 2011.

[9] S.H. Lee, M. Lee, W.J. Yoon, Y. Kim, "Frost growth characteristics of spirally-coiled circular fin-tube heat exchangers under frosting conditions," *Int. Journal of Heat and Mass Transfer,* Vol.64, pp.1-9, 2013.

[10] J.S. Wang, W.J. Luo, S.P. Hsu, "Transient

Response of s Spiral Fin with its Base Subjected to the Variation of Heat Flux," *Journal of Applied Sciences,* Vol.8, pp.1798-1811, 2008.

[11] P. Pongsoi, S. Pikulkajorn, C.C. Wang, S. Wongwises, "Effect of fin pitches on the air-side performance of crimped spiral fin-and-tube heat exchangers with a multipass parallel and counter cross-flow configulation," *Int. J. Heat Mass Transfer*, Vol.54, pp.2234–2240, 2011.

[12] P. Pongsoi, S. Pikulkajorn, C.C. Wang, S. Wongwises, "Effect of number of tube rows on the air-side performance of crimped spiral fin-and-tube heat exchangers with a multipass parallel and counter cross-flow configuration," *Int. J. Heat Mass Transfer,* Vol.55, pp.1403–1411, 2012.

[13] P. Pongsoi, S. Pikulkajorn, S. Wongwises, "Effect of fin pitches on the optimum heat transfer performance of crimped spiral fin-and-tube heat exchangers," *Int. J. Heat Mass Transfer,* Vol.55, pp.6555–6566, 2012.

[14] P. Pongsoi, S. Pikulkajorn, S. Wongwises, "Experimental study on the air-side performance of a multipass parallel and counter cross-flow L-footed spiral fin-and-tube heat exchanger," *Heat Transfer Eng.,* Vol.33, pp.1–13, 2012.

[15] P. Pongsoi, P. Promoppatum, S. Pikulkajorn, S. Wongwises, "Effect of fin pitches on the air-side performance of L-footed spiral fin-and-tube heat exchangers," *Int. J. Heat Mass Transfer,* Vol.59, pp.75–82, 2013.

[16] P. Pongsoi, S. Wongwises, "Determination of fin pitches for maximum performance index of L-footed spiral fin-and-tube heat exchangers," *J. Therm. Eng.* Vol.1, pp.251–261, 2015.

[17] P. Kiatpachai, S. Pikulkajorn, S. Wongwises, "Air-side performance of serrated welded spiral fin-and-tube heat exchangers," *Int. J. Heat Mass Transfer* Vol.89, pp.724–732, 2015.

[18] P. Kiatpachai, A. Suksangpanomrung, P. Thiangtham, C. Keepaiboon, W. Duangthongsuk, S. Wongwises, "Effect of fin efficiency models on air-side performance of crimped spiral fin-and tube heat exchangers" SAU Journal of Science & Technology, Vol.4, No.2, pp.36-55, 2018.

[19] K.A. Gardner, "Efficient of Extended Surface," *ASME Trans.,* Vol.67, pp.621, 1945.

[20] W.M. Kays, A. London, Compact heat exchangers, 3rd Ed., Mcgraw-Hill, New York, 1984.

[21] ANSI/ASHRAE Standard 33-2000, Method of Testing Forced Circulation Air Cooling and Air Heating Coils, 2000.

Author's history:

Dr. Parinya Kiatpachai is a lecturer of mechanical engineering at Department of Mechanical Engineering, Academic Division, Chulachomklao Royal Military Academy (CRMA). He received his D.Eng. in mechanical engineering from the King Mongkut's University of Technology, Thonburi, Bangmod, Thailand. His current research interests include the heat transfer performance and flow characteristics of fin-and-tube heat exchangers.

Asst.Prof.Dr. Anotai Suksangpanomrung is a assistant professor and head of mechanical engineering at Department of Mechanical Engineering, Academic Division, Chulachomklao Royal Military Academy (CRMA).

Mr. Phubate Thiangtham is a MD & Project Manager at Thai-Ingenieur Co., Ltd. He received his M.Eng. in mechanical engineering from the King Mongkut's University of Technology, Thonburi, Bangmod, Thailand.

Mr. Chanyoot Keepaiboon is a MD & Project Manager at Thai-Ingenieur Co., Ltd. He received his M.Eng. in mechanical engineering from the King Mongkut's University of Technology, Thonburi, Bangmod, Thailand.

Assoc.Prof.Dr. Weerapun Duangthongsuk is a associate professor of mechanical engineering at Department of Mechanical Engineering, Southeast Asia University (SAU). His research interests include heat transfer, fluid mechanics, and nano fluids.

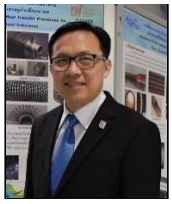

Prof.Dr. Somchai Wongwises is a professor of mechanical engineering at King Mongkut's University of Technology, Thonburi, Bangmod, Thailand. He received his Doktor-Ingenieur (Dr.-Ing.) in mechanical engineering from the University of Hannover, Germany, in 1994. His research interests include two-phase flow, heat transfer enhancement, and thermal system design. He is the head of the Fluid Mechanics, Thermal Engineering and Multiphase Flow Research Laboratory (FUTURE).